Studies On An Inert Gas Disk Hall Generator Driven In A Shock Tunnel

Author(s): Jean F. Louis

Session Name: Nonequilibrium MHD Power Generation and Stability Problems

SEAM: 8 (1967)

SEAM EDX URL: https://edx.netl.doe.gov/dataset/seam-8

EDX Paper ID: 226

STUDIES ON AN INERT GAS DISK HALL GENERATOR DRIVEN IN A SHOCK TUNNEL

Jean F. Louis
Principal Research Scientist
Avco Everett Research Laboratory
Everett, Massachusetts

Abstract

A theoretical and experimental study of the plasma properties and fluid mechanics of a large disk magnetohydrodynamic generator driven by high temperature argon seeded with cesium is presented. With a high initial degree of ionization of the seed, theoretical and experimental results indicate a quiescent behavior of the plasma and the generator performance matches the expectation based on the local values of conductivity and Hall coefficient. With a low initial degree of the seed, nonequilibrium ionization is experimentally observed but is accompanied, as theoretically expected, by large electron density fluctuations. The existence of a long relaxation length, and of density fluctuations lead to a reduction of the generator performance. The maximum effective Hall coefficient is found to be equal to two as could theoretically be expected for a plasma with large isotropic fluctuations.

I. Introduction

This paper presents the results of a theoretical and experimental study of the plasma properties and fluid mechanics of a disk generator driven by high temperature argon seeded with cesium. A two-temperature plasma can readily be achieved in such a gas by a fast expansion or by the presence of the strong electric field induced by the motion of a supersonic flow through a large magnetic field. The object of this investigation was to determine the optimal Hall coefficient, Mach number, and electron temperature for two-temperature generator operation. To obtain an understanding of the plasma and fluid mechanics, great care was taken to obtain uniform conditions. Boundary layer effects were minimized by the use of large mass flows (10 kg/s) and the symmetry of the disk eliminated the need for the axially located electrodes found in linear generators.

Section II briefly describes a theory of the disk Hall generator's operation and the character of its flow under ideal conditions. However, ideal conditions of uniform electron concentrations are not likely to exist in a two temperature plasma. A number of theories and experiments have shown that acoustic and ionization instabilities can exist in a plasma operating at Hall coefficients larger than one. These ionization instabilities lead to the presence of large electron density fluctuations which induce E x B drifts. The drifts result in a net second order current, and influence the magnitude of the average current flowing through the plasma. The analysis of Yoshikawa and Rosel (for the anomalous diffusion of a plasma across a magnetic field) was used to determine an expression for Ohm's law for the average current, assuming the r.m.s. value of the electron density fluctuations.

A nonlinear stability analysis was made to determine the r.m.s. value of the electron fluctuation in a two temperature plasma for different values of the Hall coefficient. As seeded argon at electron temperatures above $2500^{\rm O}{\rm K}$ is used, the following analysis was made with the assumption that the Coulomb collisions predominate. The analysis indicates that for electron temperature between 2500-3500°K, the ionization instability develops for Hall coefficients slightly larger than 2. For values of $\omega\tau(>3)$, the fluctuations are very large and the ratio of the effective to local conductivities is a number like $\frac{8}{\pi\omega\tau}$,

and the effective Hall coefficient tends to a value comparable to $8/\pi$. The results of this analysis are compared with published experimental data and indicate agreement.

Section III considers the main factors considered in the determination of the experimental techniques. To allow maximum flexibility in gas temperature, pressure, and Hall coefficient, an alkali shock tube was used as a high temperature gas generator. The diameter of the shock tube was chosen to obtain large mass flows and high Reynolds numbers to reduce boundary layer effects. A 3 Tesla magnet was used to obtain predominant Lorenz forces, rapid relaxation into a two-temperature plasma, large Hall effects and substantial changes in the electrical and thermodynamic properties of the gas.

Section IV reports on the experimental results. Emphasis was first placed on determining the electron density in the plasma for different initial stagnation degrees of ionization. With a magnetic field of 3 Tesla, nonequilibrium ionization is systematically found for initial degrees of ionization between 10^{-3} to 10^{-1} of the seed. The seed concentration was 10^{-3} . For stagnation conditions of $\mathfrak Z$ 3200°K and below, large electron density fluctuations were found. It was found that the relaxation time, to nonequilibrium ionization, is relatively long for low stagnation temperatures. Voltage characteristics and internal voltage distributions of the generator are also given in this section. They indicate that $\omega \tau$ eff

A correlation between the theoretical analysis and the experimental data has been found and analysis of this correlation is continuing.

II. Theoretical Aspects Related to the Flow and the Plasma Properties

A. MHD Flow Through a Disk Generator

The flow in the Hall disk generator is outward, the magnetic field is perpendicular to the plane of the disk and the electrodes are located at the inner and outer radii. The induced emf,

Work supported by: Aerospace Research Laboratories, Office of Aerospace Research; and Aeropropulsion Laboratories, Aerospace Power Division, Systems Engineering Group (RTD) Wright-Patterson Air Force Base, Ohio; under Contract AF 33(615)-3413

resulting from the motion of the gas through the magnetic field, is shorted and a Hall field (E) exists in the direction of motion. The equations

Radial Momentum:

$$\rho v_{r} \frac{dv_{r}}{dr} - \rho \frac{v_{\theta}^{2}}{r} = \frac{dp}{dr} + j_{\theta} B \qquad (1)$$

Tangential Momentum

$$\rho v_{r} \frac{dv_{\theta}}{dr} + \rho \frac{v_{\theta} v_{r}}{r} = j_{r} B$$
 (2)

$$\rho v_{r} d \left(h + \frac{v^{2} \theta + v^{2}}{2} \right) = E j_{r}$$
(3)

Conservation of Current:

$$2 \pi r j_r z = I \tag{4}$$

Conservation of Mass:

$$\rho v_{x} r z = M \tag{5}$$

Ohm's Law Along Radius:

$$j_r = \sigma E + \sigma v_{\theta} B - \omega \tau j_{\theta}$$
 (6)

The Tangent:

$$j_{\theta} = - \sigma v_{r} B + \omega \tau j_{r}$$
 (7)

where ρ is the gas density; p, pressure; v_r , v_θ , radial and tangential velocities; j_r and j_θ , radial and tangential current densities; h, the enthalpy; B, the magnetic field; E is the radial electrical field; z is the disk height; I is the total radial electrical current; and M is the mass flow; σ is the electrical conductivity and ωau is the Hall

A simple solution of practical importance can be easily derived to indicate the nature of the flow through the disk generator. This solution assumes constant static temperature dh = dT = 0. At high efficiency, the static pressure drop is very small. With the gas temperature and density being close to constant, σ and $\omega\tau$ can be considered as constant in an equilibrium generator. This generator operates as an impulse turbine with high power density and high Hall coefficient.

For a channel with no pre-rotation at the inlet, located at r = 1

$$\begin{cases} v_{\theta} = \frac{IB}{M} \left[1/r - r \right] \\ v_{r}^{2} = \frac{EM}{I} - \left(\frac{IB}{M} \right)^{2} \left[\frac{1}{8r^{4}} + r^{2} + C \right] \end{cases}$$
(8)

$$v_{r}^{2} = \frac{EM}{I} - \left(\frac{IB}{M}\right)^{2} \left[\frac{1}{8r^{4}} + r^{2} + C\right]$$
 (9)

C being the constant of integration. This solution indicates a linear dependence of the swirl upon r. With σ and $\omega\tau$ constant, Eq. (1) becomes a linear differential equation in which ρ can be readily integrated. Such an analytical solution is useful in determining the general dimensions of a disk

generator and examining the deleterious effect of swirl on the generator's performance. The expression for the short circuit current can be derived from Eqs. (6) and (7)

$$j_{\mathbf{r}} = \frac{\sigma \left[v_{\theta} B + \omega \tau \ v_{\mathbf{r}} B \right]}{1 + (\omega \tau)^{2}} \simeq (10)$$

 $(n_{\alpha} e v_{\tau} at high values of \omega \tau)$

It indicates that the short circuit current is a measure of the electron density when the velocity is known.

Effective Ohm's Law in a Partially Ionized Plasma with Electron Density Fluctuations

 1. Plasma with Electron Density Fluctuations
 The measured conductivity of a partially ionized gas in the absence of a magnetic field, is in good agreement with theoretical prediction. This agreement is found to be valid regardless of whether the electron temperature is in or out of equilibrium with the background gas. the presence of a strong magnetic field, the plasma appears to behave very differently. Velikhov^{2,3} has indicated that two instabilities can exist in such a plasma when $\omega \tau > 1$. The first is the growth of sound waves in the antiparallel direction to the current, 4 and the second is the growth of an ionization instability in a plasma with small elastic losses in which the electron temperature can be different from the background gas temperature. Kerrebrock⁵ and Nedospasov⁶ have determined the growth rate and propagation velocity for the ionization instability. Experiments by Klepeis and Rosa, 7 Dethlefsen and Kerrebrock⁸ Brederlow et al, 9 and Belousov et al, ¹⁰ have indicated important electric field and electron fluctuations in two temperature plasmas in the presence of strong magnetic fields. Simultaneously, the measured conductivity and Hall coefficients have been found to be appreciably smaller than ideally expected.

The derivation of a theoretical expression giving an effective Ohm's law for the average current in a plasma with fluctuating electron densities is important to explain the above findings and to understand the behavior of cross field (MHD) devices.

In this paper, the analysis of Yoshikawa and Rose¹ (for the anomalous diffusion of a plasma across a magnetic field) is used to determine an expression for Ohm's law for the average current. The effective conductivity and Hall coefficients derived from this theory are then compared with experimental results.

2. Ohm's Law for the Averaged Current -In the presence of a uniformly applied electric field or density gradient, electron density fluctuations induce fluctuating $\overline{E} \times \overline{B}$ drifts which give a net second order current flow (eddy current). The average first order fluctuating $\overline{E} \times \overline{B}$ drifts are zero, and the magnitude of the second order term will influence the averaged current flowing through the plasma.

Yoshikawa and Rosel have determined the magnitude of this second order term, assuming a microscopically uniform plasma subjected to a homogeneous turbulence. The local electron collision frequency is assumed to vary linearly with the local electron density (Coulomb collisions predominate) and the ions are assumed to be immobile.

Making the reasonable assumptions that $\frac{S}{\omega \tau} << 1$, where $S^{1/2}$ is the ratio of the a.c., τ .m.s. value of the density to the d.c. density; and $\omega \tau$ is the Hall coefficient for the electrons as shown in Eqs. (28) and (29) of Ref. 9, yields the relations

$$J_{x} = \frac{\sigma \Sigma_{x}}{1 + (\omega \tau)^{2}} + \frac{\sigma \Sigma_{x} (\omega \tau)^{3}}{\left[1 + (\omega \tau)^{2}\right]^{2}} SI$$

$$J_{y} = \frac{\omega \tau \sigma \Sigma_{x}}{1 + (\omega \tau)^{2}} - \frac{\sigma (\omega \tau)^{2} \Sigma_{x}}{\left[1 + (\omega \tau)^{2}\right]^{2}} SI$$
(11)

where

$$I = -\frac{1}{2\omega\tau} + \left[\frac{(\omega\tau)^2 - 1}{(\omega\tau)^2}\right] 1/2 \tan^{-1} \omega\tau,$$

 $J_{\mathbf{x}}$ is the current density in the direction of the effective applied electric field, $J_{\mathbf{y}}$ is the current density normal to the applied field and σ is the conductivity. The effective field, $\Sigma_{\mathbf{x}}$, is the sum of the electric field and the term due to the electron pressure gradient.

From these relations, the following formulation for Ohm's law can be derived

$$\overline{J} + \omega \tau \left[\overline{J} \times \overline{B} \right] = \sigma \left[\overline{E} + \frac{1}{n_e e} \text{ grad } p_e \right] + \left[(\overline{E} + \frac{1}{n_e e} \text{ grad } p_e) \right] \times \frac{\overline{B}}{B} \text{ SI} \frac{(\omega \tau)^2}{I + (\omega \tau)^2}$$
(13)

where p_e is the electron pressure and n_e the average electron density. The latter term gives the second order current flow due to the fluctuating $(\overline{E} \times \overline{B})$ drift and yields the anomalous or Bohm diffusion term for low density plasmas.

From Eq. (13) one can calculate the effective Hall coefficient ($\omega \tau_{\rm eff}$) as defined by the angle between the averaged current and the applied electric field.

$$\omega \tau_{\text{eff}} = \frac{\omega \tau - \frac{(\omega \tau)^2}{1 + (\omega \tau)^2} \text{ SI}}{1 + \frac{(\omega \tau)^3}{1 + (\omega \tau)^2} \text{ SI}}$$

Figure 1 is a plot of $\omega \tau_{\rm eff}$ as a function of $\omega \tau$ for different values of S. For large fluctuations S=0.5, and for large values of $\omega \tau$ (ie $\frac{S}{\omega \tau}$ << 1), $\omega \tau_{\rm eff} \rightarrow \frac{8}{\pi}$. Therefore a saturation of the effective Hall angle would appear where high values of $\omega \tau$ and large fluctuations occur.

Similarly, the ratio of $\frac{\sigma_{eff}}{\sigma}$ can be calculated where σ_{eff} is defined as the ratio between the average current and the field in its direction.

The result is

$$\frac{\sigma_{\text{eff}}}{\sigma} = \frac{1 + \left[\frac{\omega \tau^2}{\left[1 + (\omega \tau)^2\right]} \cdot \text{SI}\right]^2}{1 + \frac{(\omega \tau)^3}{\left[1 + (\omega \tau)^2\right]} \cdot \text{SI}}$$
(15)

Large $\omega \tau$ and large fluctuations (S \rightarrow 0.5) lead to an effective conductivity which is inversely

proportional to $\omega \tau$, $\frac{\sigma_{\text{eff}}}{\sigma} = \frac{8}{\omega \tau \pi}$. This compares

well with Velikhov's result² where $\frac{\sigma_{\rm eff}}{\sigma} \approx \frac{2}{\omega \tau}$.

The limit of S = 0.5 applies only to sinusoidal fluctuations, S could be large and equal to unity for square wave disturbances.

Vedenov and Dykhne¹² have come to similar conclusions relative to the dependence of $\sigma_{\rm eff}$ and $\omega \tau_{\rm eff}$ by considering a certain distribution of segmented striation.

3. Comparison with Published Experimental Results - Figures 1 and 2 are plots of the relations (14) and (15) for values of S between the minimum of zero and the maximum of 0.5, and for $\omega \tau > 1$. The theoretical values are compared with experiments conducted in argon and seeded with a few tenths of one percent of cesium or potassium. Due to the Ramsauer effect in argon, a two temperature plasma is readily achieved. Velikhov, Nedospasov, and Kerrebrock have shown that the growth rate of instabilities, as determined from a linear theory, is large at low degrees of seed ionization but is zero when the alkali metal is fully ionized. The theoretical growth rate is also seen to increase with increasing $\omega \tau$ and with the electron temperature elevation.

Belousov et al¹⁰ report no instability for a fully ionized seed for $\omega\tau$'s up to 4 (triangular data points). Where the seed is less than 0.1% ionized, the authors report instabilities when $\omega\tau$ >1. These become turbulent when $\omega\tau$ >3. These experimental data, obtained in a plasma diode, agree with the two limits (S=0 and S=0.5) given by the theory. Also there is a consistent value of S which correlates data obtained for $\sigma_{\rm eff}$ and $\omega\tau_{\rm eff}$.

Brederlow et al 9 obtained their data on effective conductivity and Hall coefficients, in a flow of argon seeded with potassium at a temperature of 2000°K for different electron temperatures and magnetic fields. These data indicate very clearly a saturation of the effective Hall coefficient for large electron temperatures. The authors also report fluctuations of the electric field. There is no good cross correlation between data for $\sigma_{\rm eff}$ and $\omega \tau_{\rm eff}$. Also, the data for $\omega \tau_{\rm eff}$ fall slightly below the minimum bound corresponding to S=0.5. This discrepancy may be explained by local shorting of the Hall field between adjacent electrodes as shown by Fischerll using the same experimental set-up.

Klepeis and Rosa's 7 results were obtained in a disk Hall MHD generator driven by argon at 2000°K and seeded with cesium. Fluctuating electric fields are reported and values of effective $\omega \tau$ are given which would correspond to 0.1<S<0.25 for frozen equilibrium and closer to S=0.5 for nonequilibrium.

Dethlefsen and Kerrebrock⁸ have studied the magneto-acoustic and ionization instabilities in a flow tube. They have measured $\frac{\sigma_{eff}}{\sigma_{eff}}$. These

results indicate increasing values of S as the electron temperature or current density increases. This increase in S corresponds to increasing values of the theoretical growth rate of the ionization instabilities. The experimental investigation of the plasma indicated that the magnitude of the electric field fluctuation increased with the electron temperature and $\omega \tau$; the values of S vary similarly. The results for

 $\frac{\omega \tau_{\rm eff}}{\omega \tau}$ have been normalized to a ratio of 1.0 at B =0 and plotted on Fig. 2. The trend of the results is comparable to Brederlow's, again

showing smaller $\frac{\omega \tau}{\omega \tau}$ ratios as the current density or electron temperature increases. The cross correlation of the S values is better than for Brederlow's results. The use of a circular geometry⁸ leads to the circulation of small eddy currents in the B field direction. The eddy current and wall effects could easily explain the fact that some data points fall below the limiting case of S = 0.5 (for sinusoidal fluctuations).

C. Expected Amplitude of the Fluctuations in a Two Temperature Plasma

As described previously, electron density fluctuations induce E x B drifts which result in a net second order current. The circulation of this current can produce a local increase in Joule heating which can be readily transferred into ionization energy, and lead to the growth of the magnitude of the density fluctuation. For such an instability to readily develop, the elastic losses must be relatively small. This type of ionization or electrothermal instability has been studied in a linear treatment, by Velikhov, Kerrebrock, and Nedospasov. The present analysis includes the contribution from the nonlinear terms, assuming dominant Coulomb collisions. The conditions of instability, the growth rate, and the magnitude of the fluctuations are to be determined.

A homogeneously fluctuating plasma is considered; the level of turbulence being defined as the square of the r.m.s. value of the fluctuations is S. The average current \overline{J}_0 , and electric field \overline{E}_0 are related by the effective Ohm's Law; whereas the local current $\overline{J}_0 + \overline{j}$ local electrical field $\overline{E}_0 + \overline{e}$ and the local electron density $n_e = n_o$ $(1+\zeta)$ are related through the local Ohm's law. So \overline{j} , \overline{e} and ζ define the local disturbance from the average plasma conditions. From the local and effective Ohm's law the following relation evolves;

$$\frac{\vec{j}}{\sigma} + \frac{\omega \tau}{\sigma} \left[\vec{j} \times \frac{\vec{B}}{B} \right] - \zeta \frac{\omega \tau}{\sigma} \left[\vec{J}_{o} \times \frac{\vec{B}}{B} \right] \\
= \vec{e} + \frac{k T_{eo}}{n_{o} e} \operatorname{grad} \zeta - \zeta \left[\vec{E}_{o} \times \frac{\vec{B}}{B} \gamma \right]$$
(16)

where ($\omega \tau$), σ , and T_{eo} are the average values of Hall coefficient, conductivity and electron tem-

perature, $\gamma = SI \frac{(\omega \tau)^2}{1 + (\omega \tau)^2}$. The last term of

Eq. (16) describes the influence of the homogeneous fluctuations on the disturbance under consideration.

The local ionization rate is obtained from the difference between the increase (from the average conditions) in Joule heating and the corresponding change in elastic collision losses, if radiation losses are neglected.

$$n_{o} C \frac{d\zeta}{dt} = \overline{e} \overline{J}_{o} + \overline{j} \overline{E}_{o} + \overline{e} \overline{j} - A \frac{d\ln A}{d\ln n_{o}} \zeta \qquad (17)$$

where
$$C = k T_{i} + 5/2 T_{eo} \left[1 + \frac{2 - \frac{n_{o}}{n_{s}}}{(3/2 + \frac{T_{i}}{T_{eo}}) (1 - \frac{n_{o}}{n_{s}})} \right]$$

with k T_1 being the ionization energy and n_S the seed concentration. Inis relation makes the reasonable assumption the Saha equilibrium is maintained in the fluctuation. With A representing the elastic collision losses, or

$$A = \delta \frac{m_e}{m_s} n_e \nu 3/2 k (T_{eo} - T_s)$$

 m_e and m_s are the electron and atomic masses, ν the collision frequency, and T_s the atomic temperature; Eqs. (16) and (17) can be written:

$$n_{o} C \frac{d\zeta}{dt} = \overline{e} \overline{j} + 2 \overline{j} \frac{J_{o}}{\sigma} - A \frac{d\ln A}{d\ln n_{o}} \zeta - \frac{k T_{eo}}{n_{o} e} \operatorname{grad} \zeta$$

$$J_{o} - \frac{k T_{eo}}{n_{o} e} \operatorname{grad} \zeta \overline{J}_{o} + \zeta \overline{E} \times \frac{\overline{B}}{\overline{B}} \gamma \overline{J}_{o}$$
(18)

The last two terms represent the influence of all other fluctuations on the local energy balance. The average energy equation can be written:

$$JE_o + \langle \overline{e} J \rangle = A \left[1 + S \frac{d^2 \ln A}{(d \ln n_o)^2} \right]$$
 (19)

where the last term represents the average value of the collision losses associated with the electron density fluctuations.

The stability analysis can be performed by taking a Fourier component of the disturbance as

$$\zeta = X e^{i (\overline{K} \overline{Z} + (\omega_r - i \omega_i) t)}$$

applying to Eq. (18) and making use of the relations (19) and div j = curl e = 0.

First, it is found that $\overline{e} \overline{j} = \langle e j \rangle = 0$.

Selecting $\overline{J}_{0} = J_{0} \overline{i}_{x}$, the following relations are derived:

$$\omega_{\mathbf{r}} = \frac{\tilde{\mathbf{K}} J_{o}}{n_{o} e} \frac{k T_{eo}}{C}$$

$$\omega_{\mathbf{i}} = \frac{A}{n_{o} C} \left[\left(2 \omega \tau \frac{K_{\mathbf{x}} K_{\mathbf{y}}}{K^{2}} \frac{1 + \gamma^{2}}{1 + \omega \tau_{\mathbf{y}}} + D + \frac{20}{1 + \omega \tau_{\mathbf{y}}} \right) \left(1 + \frac{S d^{2} \ln A}{(d \ln n_{o})^{2}} \right) - \frac{d \ln A}{d \ln n_{o}} \right]$$

where

$$D = \frac{K_x K_y}{K^2} \left[-2\gamma - \omega \tau \gamma \frac{\gamma - \omega \tau}{1 + \omega \tau_y} + 2\gamma^2 \frac{\gamma - \omega \tau}{1 + \gamma^2} \right] + \frac{K_y^2}{K^2}$$

$$\left[-\gamma \omega \tau + \gamma^2 \frac{\omega \tau \gamma + 1}{1 + \gamma^2} \right] + \frac{K_x^2}{K^2} \left[-2 \gamma \frac{\gamma - \omega \tau}{1 + \omega \tau \gamma} + \frac{\gamma^2 (\gamma - \omega \tau)^2}{[1 + \omega \tau \gamma](1 + \gamma^2)} \right]$$

Eq. (14) indicates that the phase velocity is roughly proportional to the electron drift velocity multiplied by the ratio of the electron to ionization temperatures as previously shown by Kerrebrock⁵ and Nedospasov. ⁶

From Eq. (20) the neutral stability condition is obtained by making ω_i =0, and solving for S in terms of $\omega \tau$. With γ =0, the neutral stability condition becomes $\omega \tau = \frac{\mathrm{dln} \ A}{\mathrm{dln} \ n_0} \approx 2$. The latter value is correct except for large degrees of ionization of the seed close to unity for which $\frac{\mathrm{dln} \ A}{\mathrm{dln} \ A} >> 2$.

Equation (20) also indicates that for an initially smooth plasma, $\gamma=0$, the direction of maximum gorwth is at 45° to the current flow direction. Figure 3 gives the neutral stability line as a function of T_e , S, and $(\omega \tau)$. In a generator operating at $\omega \tau > 3$ and with degrees of ionization of the seed << 1, the growth rate being several orders of magnitude smaller than the flow time, the fluctuations will rapidly reach values (S=0.5). In this case growth can occur over a wide range of angles, starting from presumably randomly distributed fluctuations. It would therefore be possible that a homogeneous (turbulent) pattern of electron density fluctuations could develop. For such a plasma, and for S=0.5, the relations derived for the effective $\omega \tau$ yields $8/\pi$ and for the effective conductivity indicates a dependence of $1/\omega\tau$.

At values of $\omega\tau$ close to the stability limit, striation of the plasma can develop and Rosa's 13 analysis could be applicable in this case. This analysis indicates that the effective conductivity would vary as $1/(\omega\tau)^2$ and the value of the Hall coefficient could dip much below the value of $8/\pi$.

D. The Effect of Density Fluctuations on, and Nonequilibrium Effects in an MHD Generator

Two nonequilibrium ionization regimes, (frozen and nonequilibrium) are of interest in this study.

1. Frozen Equilibrium - Previous studies on the ionization of cesium in argon have indicated that the ionization rate is energy limited, i.e., the rate is determined by the balance between the ionization energy and the energy gathered by the electron through elastic collisions. In this concentration, frozen electron temperature and concentrations are in equilibrium and determined by using the Saha equation. The rate of recombination can be written:

$$C \frac{dne}{dt} = \frac{\delta m_e}{m_a} n_e \nu 3/2 k (T_a - T_e) \equiv A$$

where C has been defined above and C = $k T_i$ with T_i the ionization temperature.

If Coulomb collisions predominate, ν a n_e and the time constant of recombination is τ a $1/n_e$ (it appears as a two body recombination). If electron atom collisions predominate, ν can be a constant and the recombination time constant τ a $1/\ln n_e$. The flow time corresponding to one interaction length varies as $1/n_e$. It can be seen that the recombination time is equal to or longer than the flow time. Therefore, generators using the slow electron recombination or frozen equilibrium are of practical interest. The addition of Joule heating during the expansion through the generator will of course make the recombination slower or change it to ionization.

2. Nonequilibrium Ionization and Effect of Non-uniformities - The electron temperature is obtained from the energy balance.

$$J E' + A \left[1 + S \frac{d^2 \ln A}{(d \ln n_0)^2} \right] = 0$$
 (21)

where E' is the field in the plasma frame of reference. The last term represents the r.m.s. value of the elastic losses associated with the fluctuations. The influence of homogeneous density fluctuations on the Joule dissipation and on the electron temperature has yet to be investigated for the disk generator. Neglecting the tangential velocity, and using the effective Ohm's law derived above, the local Joule heating is

$$J E' = \frac{\sigma V_{r}^{2} B^{2}}{1 + \omega \tau \gamma} \left[1 + \gamma^{2} + (\omega \tau - \gamma) \frac{2 J_{r}}{\sigma V_{r} B} + \frac{J_{r}^{2}}{\sigma^{2} V_{r}^{2} B^{2}} (1 + \omega \tau^{2}) \right]$$
(22)

This indicates that the local Joule heating varies with the first power of B for large $\omega \tau$ and large fluctuations, instead of the second power as for a smooth plasma. Consequently, the relaxation length and the electron temperature will vary with the first power instead of the second power of the magnetic field or the Hall coefficient, as it does

in a uniform flow.

It is worth noting that for a striated flow, Rosa's 13 analysis would indicate saturation at high $\omega\tau$ leading to no dependence on B.

III. Design of the Magnetohydrodynamic Generator Experiment

The basic components of the experiment are the energy source, the generator channel, the magnet, and the instrumentation. The conditions which directed the choice and design of the components are described below. To satisfy the requirements of flexibility in pressure, temperature, mass flows and inexpensive operation, an alkali metal shock tube was chosen to produce the high temperature gas. The gas obtained behind the reflected shock is used to drive the generator following shock tunnel techniques. The working fluid was chosen to be argon seeded with a few tenths of one percent of cesium. The driver gas was helium. The seeding technique suspends the metal as an aerosol of roughly 0. lu size in the flowing argon gas. The details of the technique and the calibration of the shock tube have been described elsewhere. 14 The diameter of the stainless steel shock tube is 15 cm and the length is 7.5 m. The size allows flows like 11 kg/s for a few miliseconds test time. This small test time brings strict requirements on the channel design and the strength of the magnetic field. The flow time through the experiment has to be at least an order of magnitude smaller than the test time (2 ms), so that steady state conditions are achieved. A total flow time of 100 µs. or less becomes mandatory.

The strength of the magnetic field is of prime importance if MHD effect are to prevail over flow inertia and viscous effects and, if nonequilibrium is to be readily achieved. The magnetic field strength must satisfy the following requirements:

1. A ratio of the Lorenz force to the inertia force close to one, or $S = \frac{\sigma B^2 L}{\rho U} \rightarrow 1,$

where L is the generator length, ρ the gas density, and U the gas velocity.

2. A ratio of Lorenz to viscous forces much larger than one, or $H^2 = \frac{\sigma \ B^2 \ L^2}{\mu} \ ,$

where μ is the gas viscosity.

3. An electron density relaxation time for nonequilibrium short compared to the flow time of

$$\tau_{\rm r} = \frac{\frac{m_{\rm e} k T_{\rm i} \nu}{e^2 U^2 B^2} << \frac{L}{U}$$
, where e is the electronic

charge, m_{e} is the electronic mass, and ν the collision frequency.

Taking values of U=1000 m/s, ρ =0.1 kg/m³, T_i =4.5 10^{4 o}K, and L=10⁻¹ m, ν =10¹² S⁻¹, it is found that S=1 for 3.2 Tesla, whereas

 $H^2=10^5$ and $\tau_r=2.10^{-6}$ s $<<\frac{L}{U}=10^{-4}$ s. Further, the magnetic Reynolds number is very low and $\omega \tau$ can vary over a wide range (0 to 20) by changing the pressure, the degree of ionization, and the magnetic field strength.

An air core magnet made of two coils provides the required magnetic field of 3.2 Tesla. Each coil is 31.8 cm ID and 48 cm OD and has forty turn of copper ship wires. The time constant of the magnet is 35 $\mu\,\text{s}$. The resistance of the magnet matches the resistance of the full battery bank in existence at Avco Everett Research Laboratory, when connected for 600 V. The magnet is pulsed for 300 ms and the 2 ms test occurs at a time around 200 ms in a constant magnetic field. The variation of the normal component of the magnetic field in the plane of symmetry is given in Fig. 4(a) and the variation in field strength with current intensity is shown in Fig. 4(b). Thus the use of a short time greatly alleviates the problem of materials, as the heat transferred to the walls is much less than the heat of ablation of various plastic materials having good insulating properties. Because of the corrosive properties of cesium, Teflon was chosen as the wall material. The structural walls are made of glass fiber reinforced epoxy.

The method of characteristics was used to calculate the nozzle configuration needed to accelerate the flow to M=2 at the inlet of the generator. This study lead to a compromise between the length of the nozzle and the degree of velocity uniformity at the inlet of the generator. The constant temperature solution described briefly in Section II, was used in determining generators dimensions. The solution considers the kinetic energy from a reduction in Mach number 2.0 to 1.2. This solution leads to a constant height channel of 2.5 cm and a length of 7 cm. The accelerating nozzle, also an anode, is made of stainless steel. Figure 5 shows one side of the disk generator with two optical windows at different radii. Downstream of the generator section, twelve stainless steel wedges form a supersonic diffuser. The wedges serve also as spacers, which take the compression force between the two coils, and support a heated cathode. This electrode is made of thoriated tungsten and was heated to 1000°K for each test. As the cathode is cesiated by the flow of argon carrying the cesium aerosol, good electron emission was expected and obtained. The cathode is located at a radius where the magnetic field is practically nil to avoid any Hall effect and at a distance of 4.5 cm from the outlet of the generator to eliminate the effects of any cathode emission non-uniformities on the current distribution in the generator.

The different loads $(0.05 \text{ to } 0.35\Omega)$ are made of two concentric carbon tubes connected in series at one end, to minimize the self inductance. The stainless steel disk shaped tank is located downstream to the supersonic diffuser (Fig. 6. The outside radius of the tank determines the test time of the experiment. The end of the test time occurs when the shock reflected at the end wall of the tank penetrates the test section.

A 30 CFM Kinney mechanical pump and a 6" Kinney diffusion pump are used to obtain the desired vacuum and argon flow rate. The diffusion pump is only used to maintain a high degree of purity between runs. The large mechanical pump is used to flow the argon, seeded with cesium aerosol at fast speed to eliminate particle settling. A series of baffles and heated gauzes are used as mechanical traps. A chemical trap, located upstream to the mechanical pump is also employed.

After more than 200 runs, the channel's teflon walls were carefully examined. Machining marks were found to be unaltered and no sign of ablation was observed around the protruding voltage potential probes or around the wedges. The existing high shear flow increases the heat transfer rate around these flow obstacles. It is concluded that no apparent ablation of the insulator occurs.

The instrumentation of the generator consists of floating potential probes, a pressure tranducer, and photomultipliers, filters with optics and interference filters to measure the continuum at 4910°A. The continuum intensity is a measurement of the square of the electron density. The cross section of this process has been determined by Mohler 15 and more recently by Agnew and Summers. 16

IV. Experimental Results

A. Objectives

The theoretical discussion in Section II indicated that a two temperature plasma could assume three different behaviors:

- 1. Plasma with Uniform Electron Temperature In this case the local conductivity and Hall coefficient can be used to describe the microscopic properties of the plasma. The Joule heating and power output vary with the square of the magnetic field for a given value of the electron temperature.
- 2. Plasma with an Isotropic or Random Distribution of Electron Density Fluctuations The particular analysis of Vedenov and Dykhne, 12 together with the application of Yoshihawa and Rose, indicate that the effective conductivity varies as $\sigma/\omega\tau$ for large values of $\omega\tau$, and that the effective Hall coefficient saturates at a value close to two for large electron density fluctuations. The Joule heating and power output become linear fluctuations of the magnetic field strength for a given electron temperature.
- 3. Striated Flow The electron temperature elevation is concentrated in striations of a length comparable to the device. As shown by Rosa, 13 the effective conductivity varies as $\sigma/\omega \tau^2$, $\omega \tau_{\rm eff}$ can assume very small values.

The purpose of the experiment has been to determine which of the above behaviors describes the plasma for a given combination of Mach number, electron temperature, and Hall coefficient.

B. Initial Conditions

For the experiment under consideration, the thermodynamic conditions of interest are stagnation pressure in the range of 10 atm and temperatures of 2000-4000°K. For optimal simulation, it is important that the gas be in equilibrium prior to its expansion through the generator. The upper curve shown in Fig. 7 gives the ionization time behind the reflected shock as a function of 1/T, for an initial pressure of 50 Torr and a cesium concentration of 10-3. Using binary scaling of the upper experimental curve, the ionization time can be calculated for the operating conditions between 2000°K and 4000°K. The predicted ionization time is much smaller than the test time of 2 ms, and even comparable or smaller than the flow time of 100 µ's. At the low temperature end, the shock tube being far from the black body, the initial electron temperature can be depressed compared to the gas temperature due to resonance radiation losses. The difference is about 2000K at 2000°K and has been reported previously. 14

C. Experiments with Initial Frozen Equilibrium

The experiments were run at a stagnation pressure of approximately 10 atm and temperatures of $4000^{\rm O}{\rm K}$ and $3200^{\rm O}{\rm K}$. For these conditions, the electron densities were calculated to be $6{\rm x}10^{14}$ and 2.5 x 10^{14} at the generator inlet for the $4000^{\rm O}{\rm K}$ and $3200^{\rm O}{\rm K}$ conditions, whereas the static gas temperature dropped to $1600^{\rm O}{\rm K}$ and $1200^{\rm O}{\rm K}$ respectively. The inlet Mach number is 2.0. The inlet values of $\omega\tau/{\rm B}$ should be 2.3 and 3.6 for $4000^{\rm O}{\rm K}$ and $3200^{\rm O}{\rm K}$ respectively.

Figure 8 gives the data obtained for a run in which an electrical output of 720 KW was measured. This power output represents 10% of the enthalpy flux. The conditions behind the reflected shock were 8.9 atm and 4000°K. The noninductive load was 0.058 Ω . The first picture in Fig. 8 indicates the test occured during magnet excitation and in a steady magnetic field. The second picture shows the free bound continuum radition. It indicates that during the test time, the square of the electron density is quasi-constant. The measured electron density is 2.85 x 10^{15} electrons/cm³. This would indicate that, due to Joule heating, the electron density has increased from the calculated level of 6×10^{14} to 2.85 x 10^{15} electrons/cm³. Concurrently, the value of $\omega \tau / B$ has been reduced from 2.3 to 0.8, yielding $\omega \tau = 2.2$. The third picture shows traces of the measured voltage potentials by the four probes located at different radial locations relative to ground, and of the generator output voltage on the load of 0.058. All signals are relatively clean from noise, during and after the test time. Figure 9 shows the radial voltage distribution through the generator. A uniform electric field is shown to exist throughout the generator. The voltage distribution also indicates that zero or a very small electrode drop occurs, although the axial current is 30 A/cm². This and other tests have demonstrated the good performance of the generator and of the experimental facility as a whole.

The open and short circuit ends of the voltage characteristics (Fig. 10) are of interest. Close to open circuit, the initial voltage distribution shows a kink followed by a voltage gradient which together with the reading from the Kistler gauge, indicates a choking or stall in the channel. A similar result was observed by Patrick and Brogan¹⁷ in a similar experiment run in argon. It is concluded that the flattening of the voltage characteristic close to open circuit conditions can be explained by choking in which leads to a reduction in the electric field associated with the subsonic flow.

The voltage characteristic shows that the voltage decreases as the current approaches its short circuit value, this results from a drop in Joule heating, electron temperature, and an increase in the generator impedance. This part of the characteristic is unstable, and the generator will settle down in the frozen regime for which the internal resistance is constant. The development of the instability is illustrated in Figs. 11(a) and 11(b) where it can be seen that the voltage potential switches from one mode to another after 1 ms. These data are supported by the direct measurement of electron density which shows a plasma close to complete seed ionization during the first milisecond, and to the initial frozen level of ionization at a later time.

Figure 12 gives the generator power output at 4000°K and a stagnation pressure of 8.9 atm. A linear dependence of the power output on the square of the magnetic field strength, and the absence of electron density fluctuations indicates that the generator's operation is close to ideal; although the electron density has been raised from its frozen level. It should be noted that $\omega \tau$ was relatively low = 2.2 in most of the generator, except at the inlet where ionization occurred. These results are in agreement with the instability theory which indicates that for such a low $\omega \tau$ no instability exists. During the very short ionization period, the growth of the instability is initially slow as the degree of ionization of the seed is high and damped as $\omega \tau$ is reduced by the increasing ionization.

D. Nonequilibrium Ionization

This nonequilibrium ionization regime is covered in tests made at stagnation temperatures between 2000° and 3000°K, and inlet pressure between 10 and 17 atm, adjusted to maintain the inlet Hall coefficient at a value of the Hall coefficient close to 10.

Figure 13 gives the voltage characteristic which indicates a deterioration of the generator's performance at temperatures lower than 3000°K. This deterioration is due to: 1) a fairly long relaxation time length, in which energy is fed from the downstream section of the generator where a high degree of ionization is found; and 2) large electron density fluctuations which result in a lowering of the effective conductivity and

ll coefficient. Figure 14 compares typical traces of the continuum radiation, measuring the square of the electron density. The trace at the left was obtained at a distance of 12.9 cm from the center, and for an initial stagnation temperature of 4000°K. The electron density

is close to 3 x 10^{15} electrons/cm³ and constant in time. The middle oscillogram has two traces: the upper trace taken at 10.2 cm and the lower at 12.3 cm from the center of the disk. At the inner radius the electron density is 1×10^{14} electrons/cm³ whereas it is 1×10^{15} electrons/ cm³ at the outer radius. This clearly indicates a relaxation, and we can also see that the electron density fluctuates appreciably. The third oscillogram corresponds to a stagnation temperature of 2150°K. The upper trace indicates an initial density slightly larger than 1 x 1016 electrons/ cm³ whereas the lower trace indicates large fluctuations (S=0.5) and up to 5 x 1016 electrons/ cm3. These data clearly show relaxation, and nonequilibrium ionization levels substantially larger than the initial degree of ionization in the stagnation region.

Figures 14 and 15 show the voltage distribution as a function of distance, for a range of stagnation temperatures between 2000 and 4000°K The stagnation pressures obtained were in excess of 9 atm. Static pressures were found to decrease from 1.3 atm, corresponding to a stagnation temperature of 4000°K, to 0.6 atm at the lowest temperature. The interaction between the gas and magnetic field is reduced as the temperature is decreased. Both Figs. 15 and 16 indicate that the electron field in the downstream part of the generator remains fairly constant but that the electric field at the inlet changes sign. This means that power is absorbed by the inlet section. As shown in Eq. (10) the local short circuit current is linearly related to the local electron density ne. For E to be positive, the local current (Jr) must be larger than the shortcircuit current associated with the local electron density. Therefore, changes in the sign of the electric field may indicate that the inlet is a relaxation region where the electron density is much lower than it is further upstream. By comparing the scale distance it can be seen that the inner window was located in the relaxation region of low electron density. The relaxation length is found to icrease with decreasing temperatures. The relaxation length extends over several centimeters, whereas the theory assuming uniform plasma indicates a relaxation length of only a few millimeters. Section II indicated that electron density fluctuations would result in a Joule heating rate varying with the first power of B instead of the second power. This lower Joule heating rate could explain the longer relaxation length. Similarly, Eq. (22) indicates that in the presence of large electron density fluctuations, the Joule heating becomes a mild function of the load. ratio Joule heating at open and short circuit becomes $(\frac{8}{\pi})^2 \simeq 6$. This fact is verified by experimental evidence as plotted in Fig. 17; which shows that the electron density measurements, taken at the inner and outer windows, are fairly insensitive to the generator loading for a given stagnation temperature of 2200°K and magnetic field strength of 2.8 Tesla. The power output of the downstream section in which nonequilibrium is achieved is high (100 MW/m³) but a large fraction of this output is fed into the relaxation region.

Although loading conditions have been widely varied with values of $\omega \tau$ between 2 and 10, no ratio of E/V_rB larger than 2 has been experimentally

measured, although values comparable to 2 have often been measured at open circuit or under load. Similarly, the variation of power output for a given load does not depend on the second power of the magnetic field as found in the "frozen equilibrium" regime.

To conclude, nonequilibrium is found to exist in the disk generator but the degree of ionization has been found to greatly fluctuate (S=0.5). The trend of the data corroborates the theories developed in Section II, both as to the existence of an instability for $\omega \tau > 2$ and for the effect of the resulting nonuniformities on the generator's performance.

V. Conclusion

A. The theoretical expressions which have been derived indicate that large fluctuations due to an ionization instability would rapidily develop when $\omega \tau > 2$, and for electron temperatures between 2500 and 35000K. The effect of such fluctuations are to reduce first the effective Hall coefficient to a value comparable to $8/\pi$ and second, the ratio of the effective to local conductivities to a number like $\frac{8}{\pi \ \omega \tau}$.

B. For experiments conducted in a disk Hall generator, using large mass flows of argon seeded with cesium, the flow is dominated by magnetohydrodynamic effects, and the viscous and electrode effects are minimized. For stagnation temperatures between 2000 and 3000°K and inlet $\omega \tau = 10$, the existence of nonequilibrium was ascertained; but this nonequilibrium has been found to be associated with large electron density fluctuations. No effective values of the Hall coefficient greater than 2 have been found to date.

C. In experiments conducted at stagnation temperatures between 3000° and 4000°K, a large degree of frozen ionization exists at the generator inlet. The degree of ionization of the seed rapidly increases within the generator to become comparable to complete ionization of the seed. The electron density has been found to be constant and the power output scales with square of the magnetic field strength as ideally expected.

REFERENCES

- Yoshikawa, S. and Rose, D. J., "Anomalous Diffusion of a Plasma Across a Magnetic Field," Phys. of Fluids, Vol. 5, No. 3, March, 1962.
- Velikhov, E. P., "Hall Instability of Current Carrying Slightly Ionized Plasma," Symp. on MHD Electrical Power Generation, Newcastleupon-Tyne, Paper No. 47, (1961).
- Velikhov, E. P., Dykhne, A. M., "Plasma Turbulence due to the Ionization Instability in a Strong Magnetic Field," Proc. Sixth Inter. Symp. on Ionization Phenomena in Gases, Paris, 1963.
- McCune, James E., "Wave Growth and Instability in Partially Ionized Gases," Avco Everett Research Laboratory AMP 136, April 1964; also, Proc. Inter. Symp. on MHD Electrical Power Generation, Paris, July, 1964.
- Kerrebrock, J. L., "Nonequilibrium Ionization Due to Electron Heating," <u>AIAA J.</u>, Vol. 2, No. 6, 1072 (1964).
- Nedospasov, A. V., "Speed of Ionization Waves in Low-Temperature Plasma," Proc Inter. Symp. MHD Electrical Power Generation, Salzburg, July, 1966, Paper SN-74/97.
- Klepeis, J. and Rosa, R.J., "Experimental Studies of Strong Hall Effects and V x B Induced Ionization," Avco Everett Research Laboratory Research Report 177, September, 1964; also presented at the 5th Symp. on the Engineering Aspects of MHD, M.I.T., April, 1964.
- Dethlefsen, R. and Kerrebrock, J. L., "Experimental Investigation of Fluctuations in a Nonequilibrium MHD Plasma," Proc. 7th Symp. on the Engineering Aspects of MHD, Princeton, March 30 - April 1, 1966.
- Brederlow, G., Feneberg, W., Hodgson, R., "The Nonequilibrium Conductivity in an Argon-Potassium Plasma in a Crossed Electric and Magnetic Fields," Proc. Inter. Symp. MHD Electrical Power Generation, Salzburg, July, 1966, Paper SM-74/15.
- Belousov, V. N., Eliseev, V. V., and Shipuk, I. Ya., "Ionization Instability and Turbulent Conductivity of Nonequilibrium Plasma," Proc. Inter. Symp. MHD Electrical Power Generation, Salzburg, July, 1966, Paper SN-74/88.
- Fischer, F. W., "Experimental Determination of the Current Distribution in a Simulated MHD Generator," Proc. Inter. Symp. MHD Electrical Power Generation, Salzburg, July, 1966, Paper SM-74/20

- 12. Vedenov, A. A. and Dykhne, A. M., "The Effective Conductivity of a Plasma in a Strong Magnetic Field," Proc. Inter. Symp. MHD Electrical Power Generation, Salzburg, July 1966, Paper SM 74/94.
- Rosa, R. J., "The Hall and Ion Slip Effects in a Non-uniform Gas," Avco Everett Research Laboratory Research Report 121, December 1961; also, Phys. of Fluids, Vol. 5, pp. 1081-1090 (September, 1962).
- 14. Louis, J. F., "Studies on an Alkali Shock Tube and on an MHD Generator Wind Tunnel," Avco Everett Research Laboratory AMP 202, August, 1966; also, Proc. Inter. Symp. MHD Electrical Power Generation, Salzburg, July, 1966, Paper SM-74/172.
- Mohler, F. L., J. Res. Natl. Bur. Stds., 19, 447 (1937).
- Agnew, L. and Summers, C., "Quantitative Spectroscopy of Cesium Plasmas," Proc. VII International Conference on Phenomena in Ionized Gases, Belgrade, 22-27 August 1965.
- 17. Patrick, R. M. and Brogan, T. R., "One Dimensional Flow of an Ionized Gas Through a Magnetic Field," Avco Everett Research Laboratory Research Report 13, October, 1957; also, J. Fluid Mechanics, Vol. 5, pp. 289-309, (February, 1959).

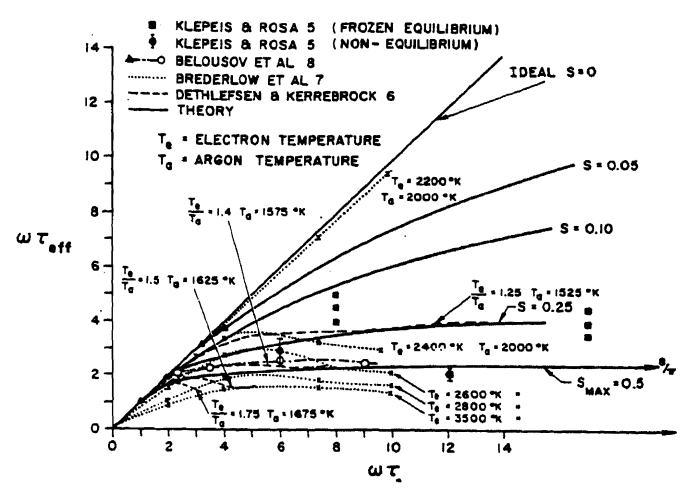


Fig. 1 Comparison of the Theoretical Expression of the Effective Hall Coefficients with Experiments as a Function of the Hall Coefficient.

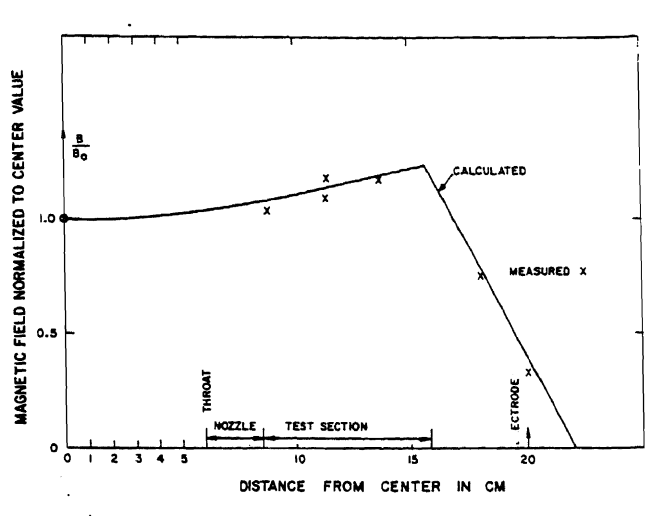


Fig. 4a Radial Distribution of Magnetic Field.

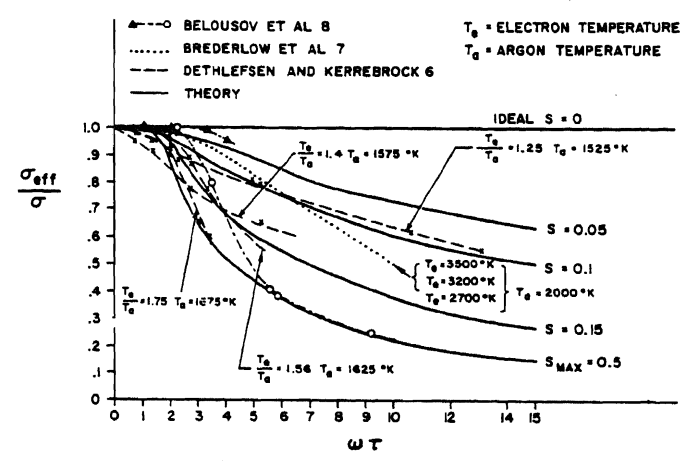


Fig. 2 Comparison of the Theoretical Ratio of the Effective to Local Conductivity with Experiments as a Function of the Hall Coefficient.

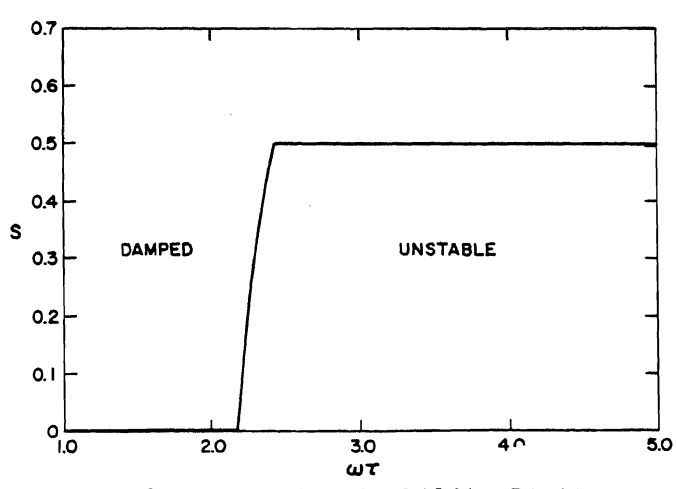


Fig. 3 Ionization Stability Limit

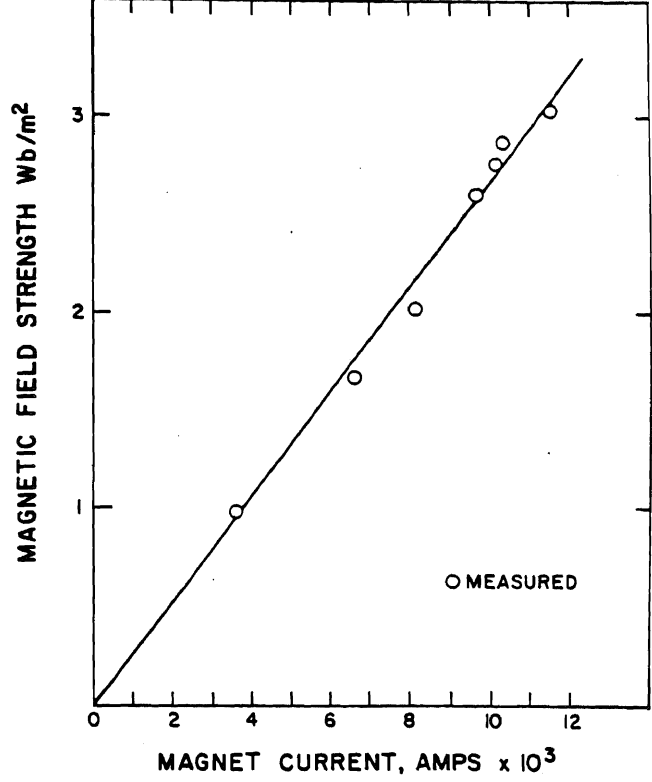


Fig. 4b Magnetic Field Strength as a Function of Magnetic Current at Center of Coils

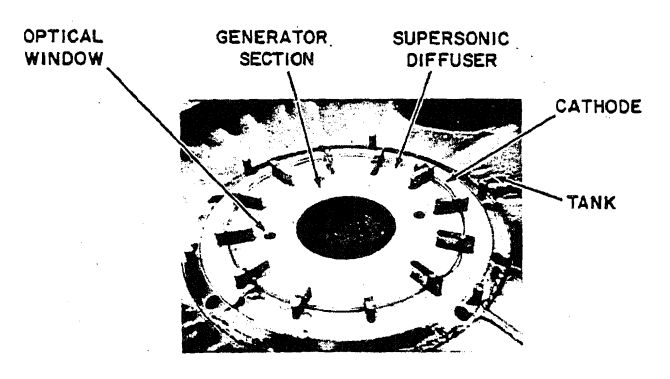


Fig. 5 View of the Dish Generator, Supersonic Diffuser and Cathode.

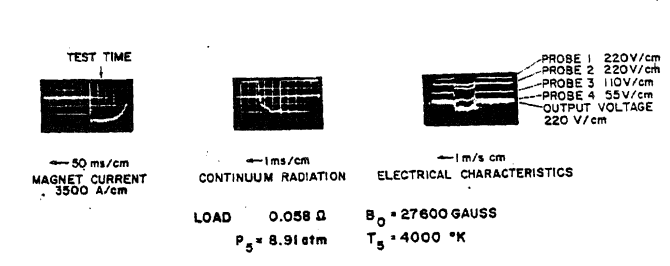


Fig. 8 Data from Run Yielding 720 kW.

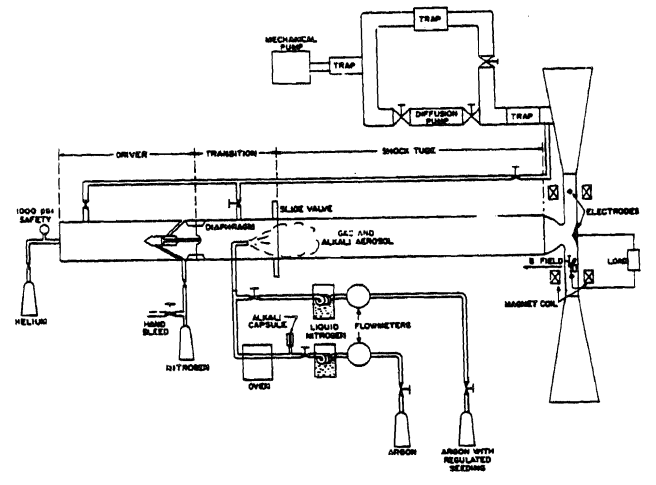


Fig. 6 Diagram of the Alkali Shock Tube and MHD Generator Wind Tunnel.

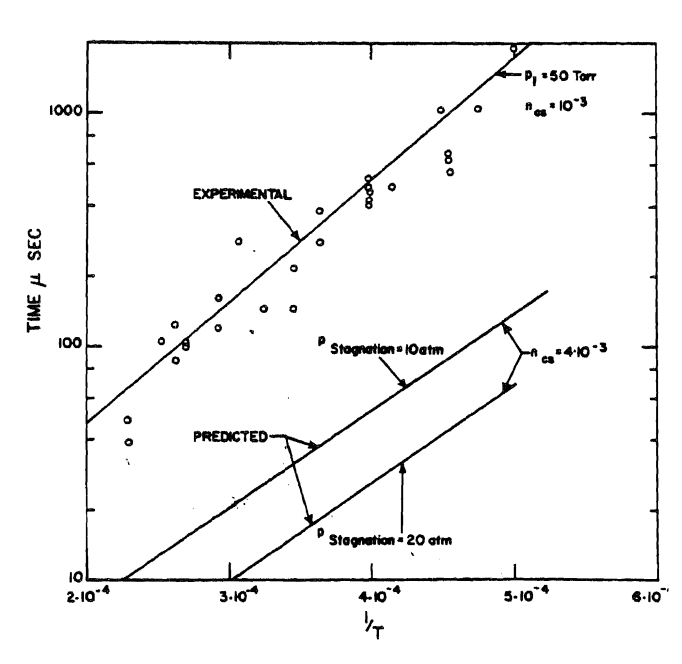


Fig. 7 Predicted and Experimental Ionization Times.

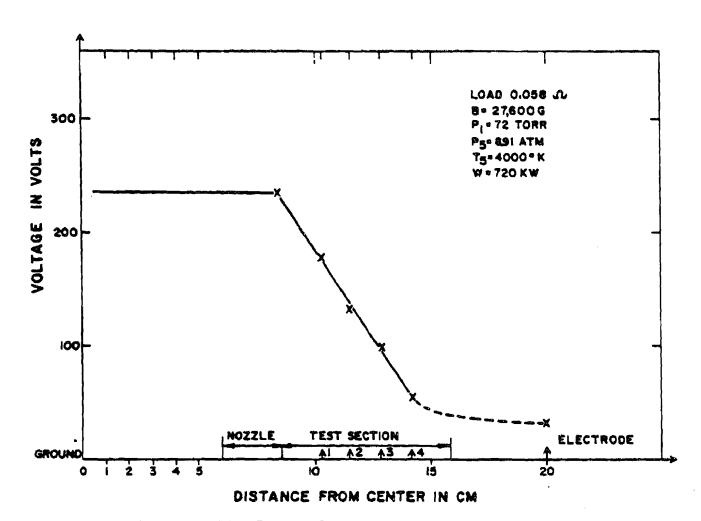


Fig. 9 Radial Voltage Distribution.

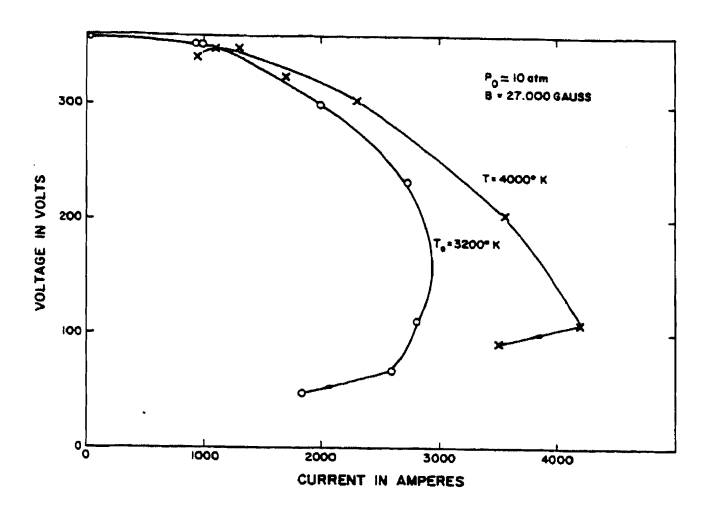


Fig. 10 Voltage Characteristics.

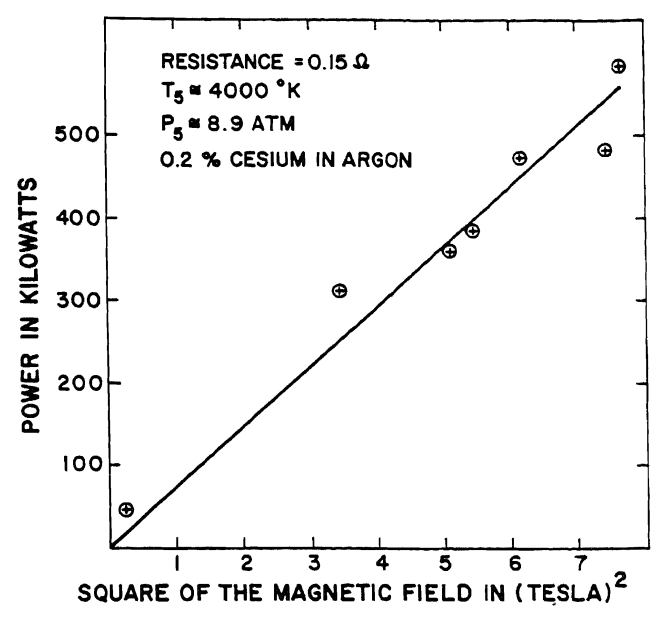


Fig. 12 Generator Power Output as a Function of the Square of the Magnetic Field.

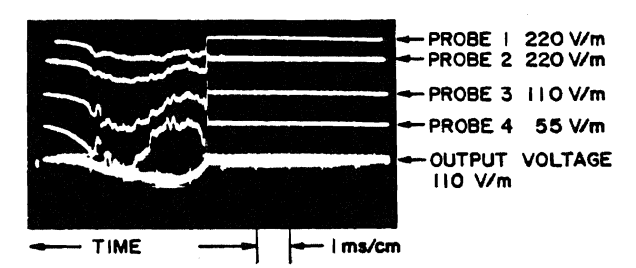


Fig. 11a Generator Voltage and Potential Probes Output.

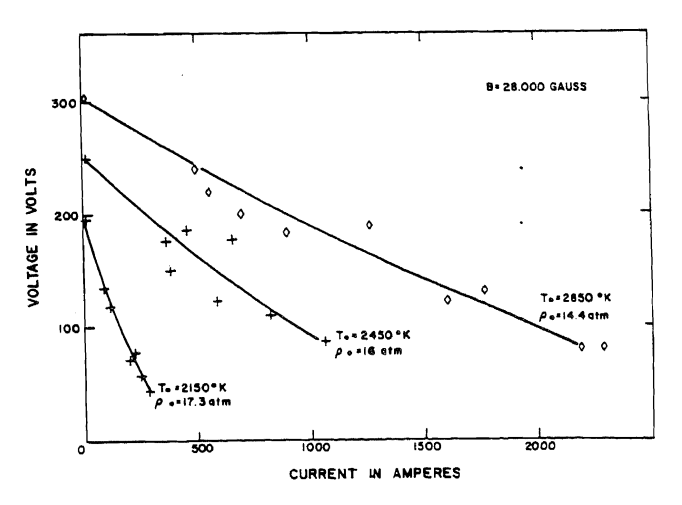


Fig. 13 Voltage Characteristics.

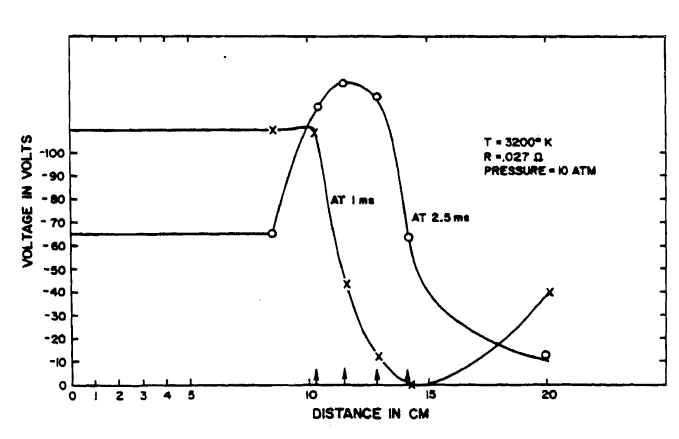


Fig. 11b Radial Voltage Distribution.

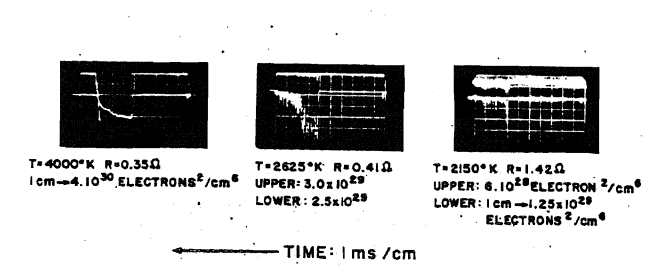


Fig. 14 Continuum Radiation Traces at Different Stagnation Temperatures.

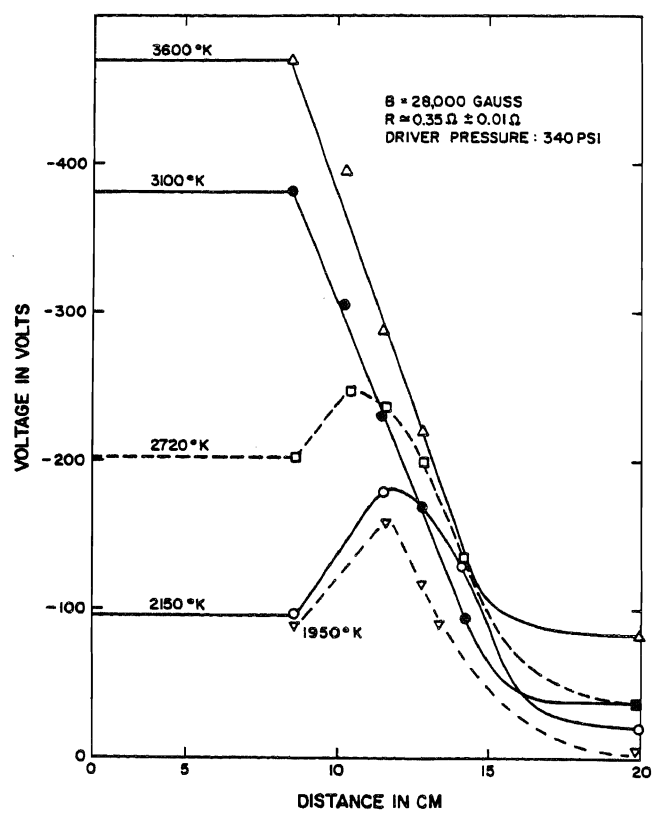


Fig. 16 Radial Voltage Distribution in the Generator for 0.35 Ω Load.

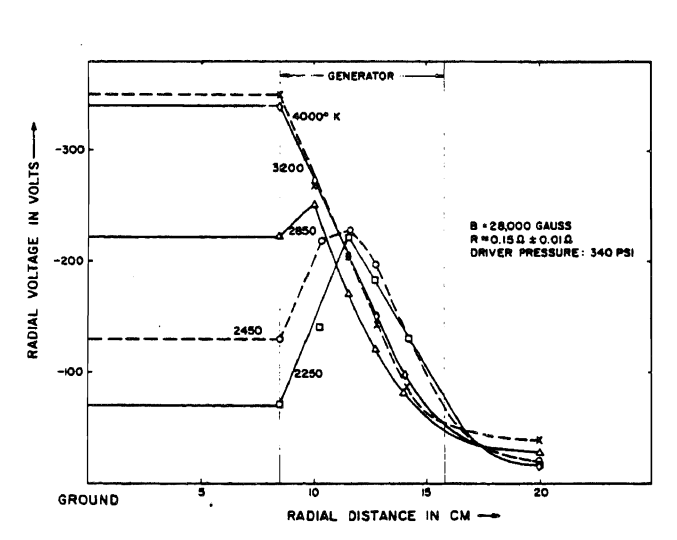


Fig. 15 Radial Voltage Distribution in the Generator for 0.15 Ω Load.

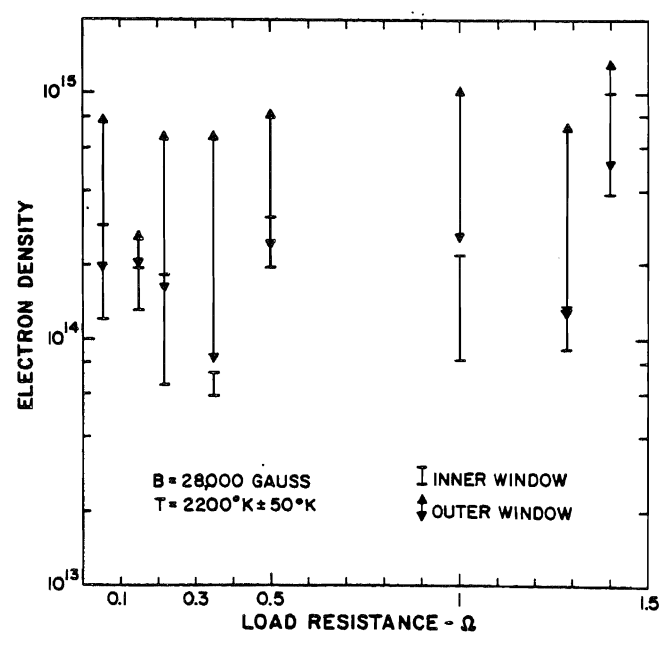


Fig. 17 Magnitude of Electron Density Fluctuations (Electrons/cm3) as a Function of the Load.